2009 Third International Conference on Power Systems, Kharagpur, INDIA December 27-29
81

Control and Protection of a Microgrid with Converter Interfaced Micro Sources

Manjula Dewadasa, Ritwik Majumder, Arindam Ghosh and Gerard Ledwich
School of Engineering Systems
Queensland University of Technology
Brisbane, Australia
jalthotage.dewadasa@student.qut.edu.au

Abstract— **This paper describes protection and control of a microgrid with converter interfaced micro sources. The proposed protection and control scheme consider both grid connected and autonomous operation of the microgrid. A protection scheme, capable of detecting faults effectively in both grid connected and islanded operations is proposed. The main challenge of the protection, due to current limiting state of the converters is overcome by using admittance relays. The relays operate according to the inverse time characteristic based on measured admittance of the line. The proposed scheme isolates the fault from both sides, while downstream side of the microgrid operates in islanding condition. Moreover faults can be detected in autonomous operation. In grid connected mode distributed generators (DG) supply the rated power while in absence of the grid, DGs share the entire power requirement proportional to rating based on output voltage angle droop control. The protection scheme ensures minimum load shedding with isolating the faulted network and DG control provides a smooth islanding and resynchronization operation. The efficacy of coordinated control and protection scheme has been validated through simulation for various operating conditions.**

Keywords- Admittance Relay, Microgrid, Islanding and Resynchronization, Active and Reactive Power sharing.

I. INTRODUCTION

The Interconnection of distributed generators (DGs) to the utility grid through power electronic converters has raised concern about system protection and smooth transfer between the grid connected and standalone modes. Parallel converters have been controlled to deliver desired real and reactive power to the system. Local signals are used as feedback to control the converters, since in a real system, the distance between the DGs may make an inter-communication impractical. The real and reactive power sharing can be achieved by controlling two independent quantities – the frequency, and the fundamental voltage magnitude [1-2]. As the converter can change the output voltage instantaneously, the load sharing can be achieved though output voltage magnitude and angle control [3]. Moreover, smooth transfer between the grid connected mode and the standalone or islanded mode is crucial in microgrid operation [4]. Either in grid connected or autonomous operation, the protection scheme has a great impact on system operation by ensuring effective fault isolation and minimum load shedding.

Protection of the microgrid is essential in both grid connected and islanded operations. Several protection issues can be identified with the connection of DGs [5]. One of the major issues is the protection in islanded operation with converter interfaced DGs [6]. The converters limit the output current during a fault. If overcurrent relays are employed to protect the system, they may not respond or take a long time to respond [7, 8]. Therefore protection of microgrid by existing overcurrent devices is a challenging task due to the current limit operation of the converter. Conventionally DGs are disconnected from the network when there is a fault in the system using an islanding detection method [9]. As per IEEE Standard 1547, DGs have to be disconnected from the electric power system for faults [10]. This may work effectively if the penetration of DGs in the system is low. However, in case of high DG penetration, the disconnection of DGs will drastically decrease system reliability.

The contribution of the paper is in enabling power sharing in a microgrid while ensuring high reliability with effective protection scheme. The current limiting operation of the voltage source converter (VSC) poses great challenge for the protection system. A new inverse time relay characteristic is proposed by using measured admittance of the protected line. The relay has the capability of isolating the faulted segment in both grid connected and islanded mode operations. Performance of designed relay is evaluated in a microgrid which has several converter connected DGs at different locations.

II. PROPOSED RELAY CHARACTERISTIC

A new inverse time relay characteristic is proposed based on admittance measurement of the protected line to avoid the drawbacks of overcurrent and distance relays. A line segment as shown in Fig. 1 is considered for this purpose. Let the relay be located at node R and let K be an arbitrary point on the line. The total admittance of the protected line segment is denoted by Y_t and measured admittance between the points R and K is denoted by Y_m. Then the normalized admittance (Y_r) can be defined as

$$Y_r = abs\left(\frac{Y_m}{Y_t}\right) \tag{1}$$

This normalized admittance is used to obtain an inverse time tripping characteristic for the relay. The general form for the inverse time characteristic of the relay can be expressed as

Queensland University of Technology, Australia

978-1-4244-4331-4/09/$25.00 Â©2009 IEEE

$$t_p = \frac{A}{Y_r^{\rho} - 1} + k \quad (2)$$

where A, ρ and k are constants, while the tripping time is denoted by t_p. These values of the constants are chosen to tune a particular relay characteristic. For example, the relay tripping characteristic for A = 0.0037, ρ = 0.1 and k = 0 is shown in Fig. 2. The normalized admittance (i.e. Y_r) becomes higher as the fault point moves towards the relay location. As a result, the relay gives a lower tripping time for a fault near to the relay. On the other hand, higher fault clearing time will ensue when the fault is further away from the relay location.

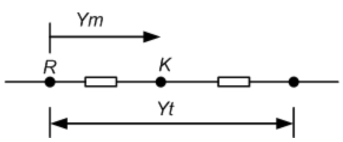

Fig. 1. Protected line segment

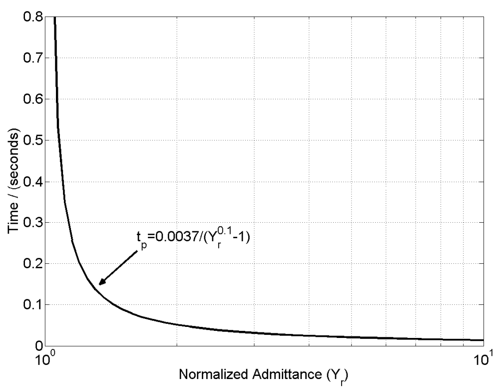

Fig. 2. Proposed relay tripping characteristic

Relay reach setting can be implemented by choosing a suitable value for the Y_t. This is totally dependent on the protection requirements such as primary and backup protections. For a particular relay, different values for Y_t can be assigned to generate a number of required zones of protection as in distance relays. For example, reach of the Zone-1 of each relay can be set as 120% of positive sequence admittance of a line segment and for the Zone-2, it can be selected as twice of the positive sequence admittance of a line segment. The proposed new relay has the ability to isolate the faults occurring at either side of a radial feeder. However for the relay to operate for reverse faults there must be an infeed from a DG that is located downstream from the relay. If the distribution network consists of these relays located at equal distances, the same forward and reverse reach can be used to isolate forward and reverse faults.

In the case of distance relays, the relay will take the same time period to issue the trip command, if the fault is within a particular zone. Moreover the relay does not consider the distance to the fault within the particular zone. On the other hand these newly designed relay have the inverse time characteristic in a particular zone. We do not need to keep a safety margin in Zone-1 in this newly designed relay to compensate errors as in the case of distance relay, since the new relay has an inverse time characteristic. Any upstream relay always provides the back up protection for the immediate downstream relay. These are the advantages of proposed relay over the conventional distance relays. In the case of overcurrent protection in a radial feeder, the relay near to the source takes longer time to operate due to the time dial setting. However in this case, the relay near to the source will take the same time to operate as other relays do. The measured admittance is the only parameter that will decide the relay tripping time. This is an advantage of proposed inverse time admittance relay over an overcurrent relay.

III. Converter Structure and Control

$DG1$ is assumed to be an ideal dc voltage source supplying a voltage of V_{dc1} to the VSC. The converter contains three H-bridges. The outputs of each H-bridge are connected to single-phase transformers and the three transformers are connected in Y. The VSC is controlled under closed-loop feedback. Consider the equivalent circuit of one phase of the converter as shown in Fig. 3. In this, $u \cdot V_{dc1}$ represents the converter output voltage, where u is the switching function that can take on values ± 1. The resistance R_T represents the switching and transformer losses, while the inductance L_T represents the leakage reactance of the transformers. The filter capacitor C_f is connected to the output of the transformers to bypass switching harmonics, while L_f represents the output inductance of the DG source. The converter structures of all the single phase DG sources are same.

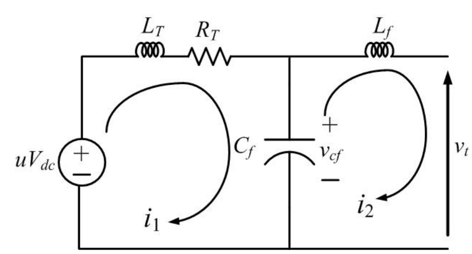

Fig. 3. Single-phase equivalent circuit of VSC.

The main aim of the converter control is to generate u. A state feedback controller used for the VSC needs three states, converter output voltage (voltage across the capacitor v_{cf}), output current and the filter current. Since magnitude and angle reference of the output voltage, V and δ are obtained from the droop equation, the reference for the capacitor voltage and current are given by

$$v_{cfref} = V\cos(\omega t + \delta) \quad (3)$$

$$i_{cfref} = V\omega C_f \sin(\omega t + \delta) \quad (4)$$

The reference for the current i_2 can be calculated as

$$i_{2ref} = \frac{v_{cf} - v_t}{jX_f} \quad (5)$$

The above equation will need a phase shifter for the calculation of the instantaneous current reference. This may not be desirable. Hence the measured values of the average real and reactive power output of the VSC can be used to find the magnitude and phase angle of the reference rms current as

$$\left|I_{2ref}\right| = \frac{\sqrt{P^2+Q^2}}{V_{cf}} \text{ and } \angle I_{2ref} = \delta - \tan^{-1}(Q/P)$$

where $V_{cf} = V$. Hence the current reference can be given as

$$i_{2ref} = \left|I_{2ref}\right| \cos\left(\omega t + \angle I_{2ref}\right) \quad (6)$$

The state feedback and the switching control laws are given as

$$u_c(k) = K\left[x^*(k) - x(k)\right] \quad (7)$$

$$\begin{aligned} &\text{If } u_c > h \text{ then } u = +1 \\ &\text{elseif } u_c < -h \text{ then } u = -1 \end{aligned} \quad (8)$$

where h is a small number. In (7), K is the feedback gain matrix and x^* is the reference state vector. In this paper, this gain matrix is designed using LQR method. How the references are set for either of the controller will be discussed in the next section.

Current Feedback for VSC connected DGs

As discussed previously when the load demand is much more than the rated output power from the DG, it is switched to a sinusoidal current limiting mode. In this mode, the droop is bypassed and the current is limited by the maximum rating of real and reactive power. Let the maximum available power rating of the i[th] DG be denoted by P_{imax} and Q_{imax}. Also note from Fig. 3 that the output voltage is denoted by $V\angle\delta$. Let the output voltage of i[th] DG is denoted by $V_i\angle\delta_i$ and reference phasor injected current passing through the inductor L_f be denoted by $I_{2iref}\angle\beta_{ref}$. Then the maximum complex power that can be supplied by the DG is

$$\begin{aligned} P_{i\max} + jQ_{i\max} &= V_i\angle\delta_i\left(I_{2iref}\angle\beta_{ref}\right)^* \\ &= V_i I_{2iref}\angle\left(\delta_i - \beta_{ref}\right) \end{aligned} \quad (9)$$

where $*$ denotes the conjugate operation. From the above equation, the magnitude and the angle of the reference current can be calculated as

$$\begin{aligned} I_{2iref} &= \sqrt{P_{i\max}{}^2 + Q_{i\max}{}^2} \Big/ V_i \\ \beta_{ref} &= \delta_i - \tan^{-1}\left(Q_{i\max}/P_{i\max}\right) \end{aligned} \quad (10)$$

The instantaneous quantities are then generated from these phasor quantities. These are then tracked using the state feedback mentioned before.

IV. Load Sharing with Angle Droop

The angle droop control strategy is applied to all the DGs in the system [3]. The output voltages of the converters are controlled to share the load proportional to the rating of the DGs.

A. Angle Droop Control and Power Sharing

Let the instantaneous real power be denoted by p and the reactive power be denoted by q. These instantaneous powers are passed through low pass filter to obtain the average real and reactive power P and Q. The average powers can then be written as

$$\begin{aligned} P &= \frac{V \times V_t \sin(\delta - \delta_t)}{X_f} \\ Q &= \frac{V^2 - V \times V_t \cos(\delta - \delta_t)}{X_f} \end{aligned} \quad (11)$$

It is to be noted that the VSC does not have any direct control over the microgrid voltage at the bus $V_t\angle\delta_t$ (see Fig. 3). Hence from (11), it is clear that if the angle difference $(\delta - \delta_t)$ is small, the real power can be controlled by controlling δ, while the reactive power can be controlled by controlling voltage magnitude. Thus the power requirement can be distributed among the DGs, similar to conventional droop by dropping the voltage magnitude and angle as

$$\begin{aligned} \delta &= \delta_{rated} - m \times \left(P_{rated} - P\right) \\ V &= V_{rated} - n \times \left(Q_{rated} - Q\right) \end{aligned} \quad (12)$$

where V_{rated} and δ_{rated} are the rated voltage magnitude and angle respectively of the DG, when it is supplying the load to its rated power levels of P_{rated} and Q_{rated}. The coefficients m and n respectively indicate the voltage angle drop vis-à-vis the real power output and the voltage magnitude drop vis-à-vis the reactive power output. These values are chosen to meet the voltage regulation requirement in the microgrid.

V. Simulation Studies

Simulation studies are carried out with a six bus microgrid system as shown in Fig. 4. The micro-grid has three converter interfaced DGs at BUS-2, BUS-4 and BUS-6. The loads are represented by *Load*_1 and *Load*_2, which are connected at BUS-3 and BUS-5 respectively. The measured admittance based protective relays, R_1, R_2 and R_3, are located at BUS-1, BUS-3 and BUS-5 respectively. Each of the DG is connected to the microgrid through a circuit breaker which provides the protection for the DG. The system parameters chosen for the study are shown in Table-I. The simulation studies demonstrate the protection of the microgrid in grid connected as well in autonomous mode, ensuring proper load sharing among the DGs.

A. Power sharing with angle droop control

Power sharing of the converters in grid connected and islanded mode operation is shown in this section. It is assumed that the system is grid connected and the DGs supply their rated power. The rest of the power demand is supplied by the grid. At 0.6 s the system goes to autonomous mode and the DGs supply the total power demand in the microgrid. The response is shown in Fig. 5. Real power supplied by the grid is denoted by P_g and real power output of each DG is shown by P_{DG1}, P_{DG2} and P_{DG3}. In this mode of operation, the VSCs shared the real power according to the angle droop control settings. At 0.8 s, microgrid is connected back to the grid and the DGs continue to supply the rated power as before. The smooth resynchronization can be achieved with proper control of the VSCs [4]. The terminal voltage of *DG*1 during the islanding and resynchronization process is shown in Fig. 6. It can be seen that the voltage of *DG*1 remains close to the rated value irrespective of the mode of operation ensuring a reliable system operation. The other DGs exhibit similar reliability in their terminal voltage in different modes of operation.

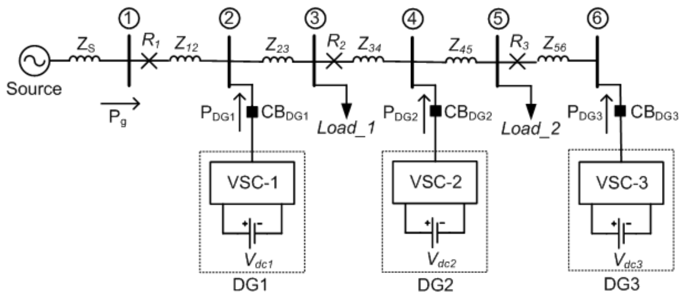

Fig. 4. Simulated microgrid system

TABLE-I: SYSTEM AND CONTROLLER PARAMETERS

System Quantities	Values
Systems frequency System voltage Line impedance(Z_{12}=Z_{23})	50 Hz 11 kV 0.3 + j 0.6283 Ω
Load ratings *Load_1* *Load_2*	 448 kW to 7 kVAr 448 kW to 7 kVAr
DG ratings (nominal) *DG*1 *DG*2 *DG*3	 300 kW 240 kW 240 kW
Output inductances L_{f1} L_{f2} L_{f3}	 3 mH 2.4 mH 2.4 mH
DGs and VSCs	
DC voltages (V_{dc1} to V_{dc4}) Transformer rating VSC losses (R_f) Filter capacitance (C_f) Hysteresis constant (h)	3.5kV 3.5kV/11 kV, 0.5 MVA, 0.1pu 3 Ω 50 μF 10^{-5}
Angle Droop Controller	
m_1	0.16 rad/MW
m_2	0.2 rad/MW
m_3	0.2 rad/MW

B. *Current limiting operation of VSCs*

To protect the converters during a fault, the output current of each VSC is limited to twice of the rated current. The limiting value of the current is 50 A for *DG*1 while *DG*2 and *DG*3 are limited to 40 A. To illustrate the current limiting operation, a three phase fault is created at BUS-3 in the microgrid at 0.4 s. Fig. 7 shows the phase a currents of all three converters and it can be seen that the current is limited within 1/2 a cycle after the fault.

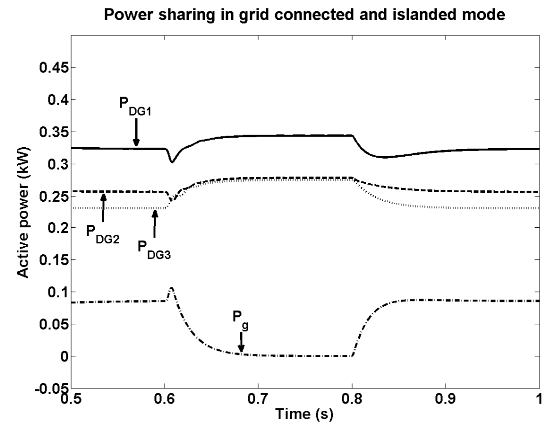

Fig. 5. Power sharing in grid connected and autonomous modes

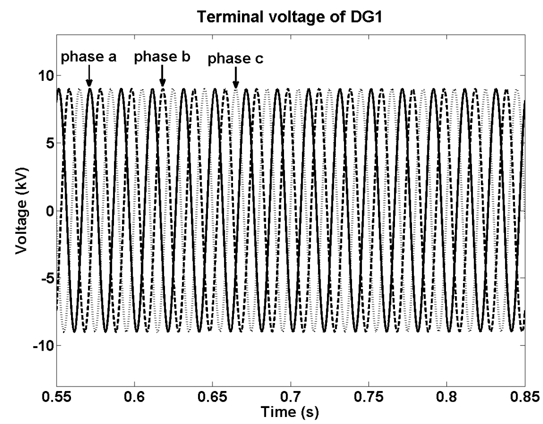

Fig. 6. Terminal voltage of *DG*1 during grid connected and autonomous mode

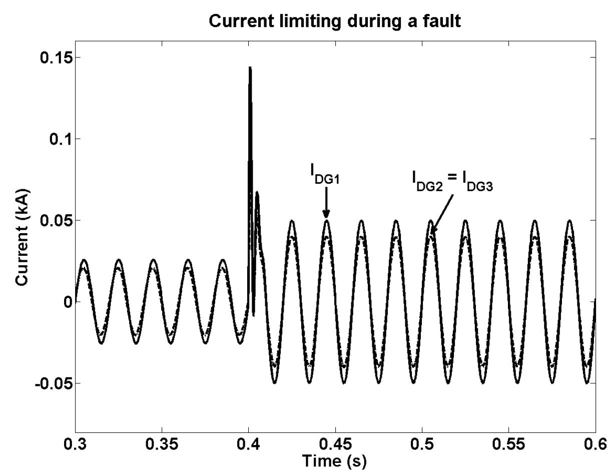

Fig. 7. Current limiting of DGs during a three phase fault

C. *Fault detection in grid connected operation*

In this section the fault detection of proposed protection scheme in grid connected mode is investigated. Once the fault is detected by a relay, the fault clearing is achieved by corresponding circuit breaker operation. At the instant of initiation the fault, all three DGs are switched into the current control mode and their output currents are limited to twice of the rated current. It is assumed that the converters can supply the high current at current limiting mode for a few cycles during the fault. Once the relay operates and isolate the fault, the DGs start operating in state feedback mode. This ensures lesser DG loss and higher reliability of the microgrid.

To investigate the efficacy of the relay response and relay co-ordination, a three phase fault is created between the BUS-2 and BUS-3 at 0.4 s, while the microgrid is running in steady state in grid connected mode. The relay R_1 at BUS-1 responds at 0.528 s to isolate the fault from grid side. After that $DG1$, $DG2$ and $DG3$ feed the fault in islanded operation. The relay R_2 responds to the fault at 0.552 s to isolate it from downstream side. But $DG1$ still feeds the fault once after the isolation of faulted segment by R_1 and R_2. Therefore the circuit breaker CB_{DG1} operates to disconnect the $DG1$ from the system. Once the fault is cleared, the microgrid which is now beyond the BUS-2, operates in autonomous mode with $DG2$, $DG3$ and *Load*_2. In autonomous mode the power sharing controller ensures a rating based power sharing of the DGs. Power sharing of each DG before the fault, during the fault and after the fault is shown in Fig. 8. The rated power output before the fault, limited power output during the fault and proportionally shared output after the fault validate the current limiting and power sharing operation of the converter interfaced DGs.

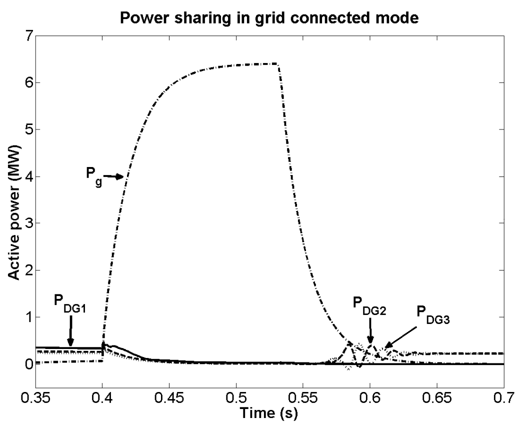

Fig. 8. Power sharing during and after a fault

D. Fault detection in islanded operation

The fault detection in islanded operation is verified in this section with the relay response and power sharing during and after the fault. It is assumed that the circuit breaker at R_1 is open and the system is running in autonomous mode. With the system running in steady state, a three phase fault is created between the BUS-2 and BUS-3 at the time of 0.4 s. The relay R_2 responds at 0.499 s to open the circuit breaker at BUS-3. $DG1$ will be disconnected by the DG circuit breaker CB_{DG1} and *Load*_1 experience a power failure. $DG2$ and $DG3$ begin to supply the power to *Load*_2. Power sharing of each of the DG during and after the fault is shown in Fig. 9. Before the fault $DG1$, $DG2$ and $DG3$ share the power as desired in 1.25:1:1 ratio. During the fault DGs limit the current in current control mode. After the successful isolation of the fault, $DG2$ and $DG3$ share the load power in autonomous mode equally.

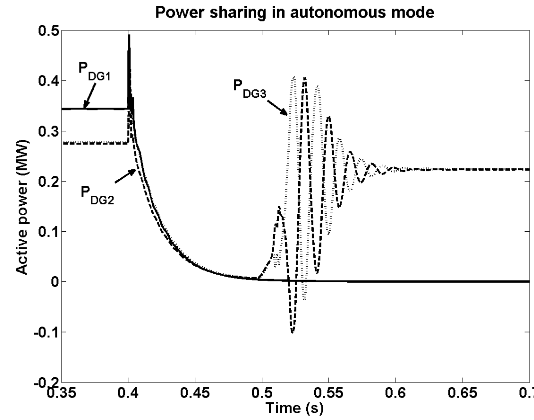

Fig. 9. Power sharing in autonomous mode during a fault

To evaluate the performance of proposed control and protection scheme in a more downstream side of the microgrid, a fault between BUS-4 and BUS-5 is considered in the islanded operation. A three phase fault is created at 0.4 s. The active power of each DG, output current of phase a and relay response are shown in Fig. 10. It can be seen from the 10(c), the relay R_3 detects the fault at 0.499 s to isolate the fault from downstream side of the microgrid. The active power and output current of $DG3$ becomes zero after the R_3 response as can be seen from Figs. 10(a) and 10(b) respectively. $DG1$ and $DG2$ continue to feed the fault in current control mode until the R_2 responds at 0.622s to isolate the fault from upstream side as shown in 10(c). After the isolation of faulted segment in the microgrid, $DG1$ supplies the power to *Load*_1 in autonomous mode. Active power output of $DG1$ has been shown in 10(a).

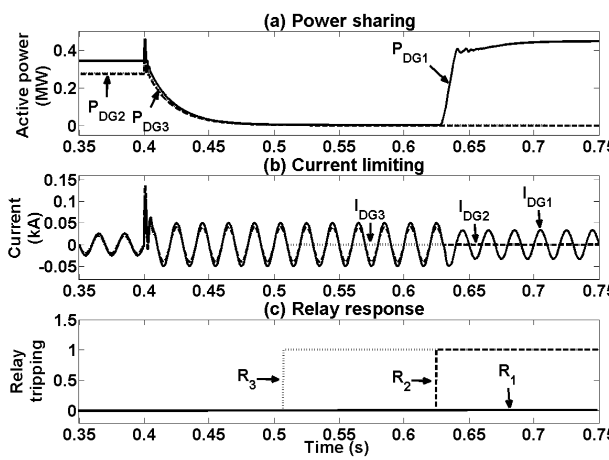

Fig. 10. Power sharing, DG currents and relay response for a fault

To verify the relay response and power sharing with the motor loads, a 425 kW three phase induction motor is connected as *Load_2* at BUS-5. Similar to the previous case, a three phase fault is generated at 0.4 s between BUS-2 and BUS-3 while the system was running in an autonomous mode. The relay R_2 responds at 0.492 s allowing $DG1$, $DG2$ and induction motor to operate in islanded mode. Power sharing of DGs during and after the fault is shown in Fig. 11(a), while real power consumptions of *Load*_1 and the motor load are shown in Fig. 11(b). It can be seen that the protection system isolates the faulted part of the network and the DGs share the real power after the fault condition in the presence of a motor load as desired.

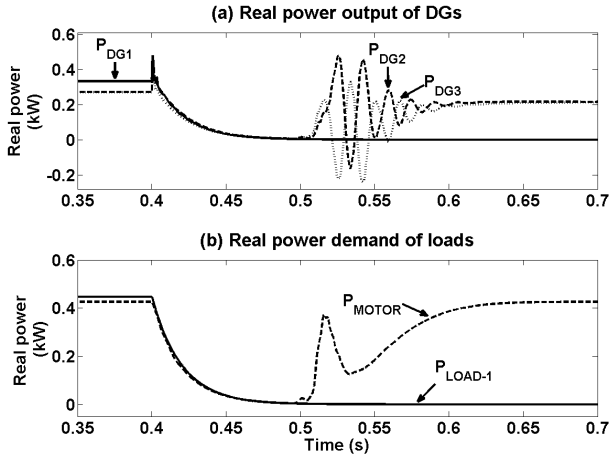

Fig. 11. Real power variation of DGs and loads during a fault

VI. Conclusion

The coordinated control and protection of a microgrid in grid connected and autonomous mode is discussed in this paper. The proposed protection scheme ensures maximum reliability of the system, while the converter control enable the DGs to share power as desired in grid connected or autonomous operation. The main challenge of the protection, due to current limiting state of the converters is overcome by using admittance relays in the proposed scheme. A stable operation in various operating condition shows the efficacy of proposed control and protection scheme.

Acknowledgement

The authors thank the Australian Research Council (ARC) for the financial support for this project through the ARC Discovery Grant DP 0774092.

References

[1] J. M. Guerrero, L. G. de Vicuna, J. Matas, M. Castilla, and J. Miret, “A wireless controller to enhance dynamic performance of parallel inverters in distributed generation systems,” IEEE Transactions on Power Electronics, Vol. 19, pp. 1205-1213, 2004.

[2] M. Reza, D. Sudarmadi, F. A. Viawan, W. L. Kling, and L. Van Der Sluis, “Dynamic stability of power systems with power electronic interfaced DG,” Power Systems Conference and Exposition, PSCE'06, pp. 1423-1428, 2006.

[3] R. Majumder, A. Ghosh, G. Ledwich and F. Zare, “Load sharing and power quality enhanced operation of a distributed microgrid,” IET Renewable Power Generation, Vol-2, No-3, pp 109-119, June, 2009.

[4] R.Majumder, A.ghosh, G. Ledwich and Firuz Zare, “Control of parallel converters for load sharing with seamless transfer between grid connected and islanded modes”, IEEE Power and Energy Society General Meeting, Pittsburgh, USA, pp 1-7, 2008.

[5] S. P. Chowdhury, S. Chowdhury, C. F. Ten and P. A. Crossley, “Islanding protection of distribution systems with distributed generators – A comprehensive survey report,” IEEE Power and Energy Society General Meeting, 2008.

[6] H. Nikkhajoei and R. H. Lasseter, “Microgrid protection”, IEEE Power Engineering Society General Meeting, 2007

[7] R. M. Tumilty, M. Brucoli, G. M. Burt, and T. C. Green, “Approaches to network protection for inverter dominated electrical distribution systems,” The 3rd IET International Conference on Power Electronics, pp. 622-626, 2006.

[8] R.H.Lasseter, "MicroGrids," IEEE Power Engineering Society Winter Meeting, vol. 1, pp. 305-308, 2002.

[9] L. K. Kumpulainen and K. T. Kauhaniemi, "Analysis of the impact of distributed generation on automatic reclosing," Power Systems Conference and Exposition, vol. 1, pp. 603-608, 2004.

[10] IEEE Std. 1547, “IEEE standard for interconnecting distributed resources with electric power system”.